

各向异性表面张力对定向凝固中深胞晶生长的影响*

陈明文^{1)†} 陈弈臣¹⁾ 张文龙¹⁾ 刘秀敏¹⁾ 王自东^{2)‡}

1)(北京科技大学数理学院, 北京 100083)

2)(北京科技大学材料科学与工程学院, 北京 100083)

(2013年8月29日收到; 2013年11月5日收到修改稿)

利用匹配渐近展开法和多变量展开法求出定向凝固深胞晶生长的浓度场和界面形态的全局渐近解, 研究各向异性表面张力对定向凝固深胞晶生长的影响。结果表明, 各向异性表面张力对定向凝固过程深胞晶生长有显著的影响。随着各向异性表面张力增大, 胞晶前端部分浓度减小而胞晶界面收缩; 胞晶根部的浓度增大而界面曲率增大或根部的曲率半径减小, 各向异性表面张力使得深胞晶界面振幅增加。本文结果能够计算定向凝固过程中深胞晶生长的浓度、界面形态。

关键词: 定向凝固, 深胞晶, 各向异性表面张力, 渐近解

PACS: 81.10.Aj, 81.30.Fb

DOI: 10.7498/aps.63.038101

1 引言

在定向凝固过程中典型的固液界面微结构形态是胞晶和枝晶。当拉速 V 充分小时, 固液界面是平直的; 随着拉速 V 的增加, 平直的界面变成弯曲的小振幅胞晶界面; 当拉速 V 进一步增加时, 界面演化变成振幅较大的深胞晶。当拉速 V 进一步增加并超过某个临界速度 V_c 时, 深胞晶界面演化变成枝晶界面。当进一步增加拉速 V , 枝晶界面演化变成平直界面。对振幅较小的胞晶界面以及对枝晶界面, 经过半个多世纪的深入研究, 先后形成了 M-S 不稳定性理论^[1,2]、微观可解性条件^[3–7]和界面波理论^[8]等, 例如 Langer 等^[3]作了对称理论模型的稳定性分析。Corell 和 McFadden 等^[4–7]将两相的热物理性质参数视为不同, 研究非对称模型的界面形态稳定性, Davis^[9]总结了凝固过程中晶体界面形态微结构的研究工作, 黄卫东等^[10]实验发

现在定向凝固过程中胞晶的形态选择具有历史相关性, 深化了对定向凝固界面微结构的认识。张云鹏等^[11]采用 CA 方法模拟界面能各向异性对胞晶生长形态的影响, 发现界面能各向异性强度会显著影响稳定胞晶的形态。对于扰动振幅较小的胞晶界面, 在临界速度 V_c 附近的平直界面上以振幅作为小的扰动参数展开, 在此基础上可以作线性和弱非线性稳定性分析, 但当拉速 V 超过临界速度 V_c 后进一步增加, 凝固系统的扰动充分发展, 界面变成指状结构, 其胞晶的根部加深使胞晶界面变为深胞晶, 其界面扰动振幅变大而不能以振幅作为扰动参数展开, 因而线性和弱非线性理论不再有效。Weeks 和 Saarloos 等^[12,13]用渐近匹配方法研究了深胞晶界面结构的性质和界面形态稳定性, 指出守恒律对于深胞晶根部封闭的重要性, 但是这些理论分析没有能够求出在深胞晶根部的解析解, 因而不能确定整个胞晶的界面形态、尖端位置和根部位置、深胞晶的振幅、前端的溶质浓度分布以

* 教育部海外名师项目(批准号: MS2010BJKJ005)、国家自然科学基金(批准号: 10972030)和中央高校基础研究基金(批准号: FRF-BR-11-034B)资助的课题。

† 通讯作者。E-mail: chenmw@ustb.edu.cn

‡ 通讯作者。E-mail: wangzd@mater.ustb.edu.cn

及这些数学量之间的解析关系. Chen 等^[14]研究 Hele-shaw 生长室中在各向同性表面张力作用下深胞晶生长形态, 利用匹配渐近展开法得到了整个深胞晶形态的近似解析解, 揭示了深胞晶界面形态有低频不稳定性和震荡全局不稳定性两种物理机理. 本文在 Chen 等^[14]在各向同性表面张力作用下深胞晶生长研究的基础上, 利用匹配渐近展开法和多重尺度法获得了定向凝固深胞晶生长的浓度场和界面形态的渐近解, 进一步研究各向异性表面张力对定向凝固中深胞晶生长形态的影响.

2 深胞晶生长的数学模型

考虑二元合金熔体定向凝固过程中的深胞晶生长, 其液相位于上半空间, 界面拉伸速度为常数速度 V , 方向指向向上液相方向. 假定固相是相对静止的, 在随界面向上移动且原点位于胞晶尖端的直角坐标系 Oxy 中, 温度梯度为 G_T , 远场浓度为 C_∞ , 胞晶列的周期为 ℓ_w . 深胞晶生长满足热传导方程、溶质扩散方程、界面方程, 包括热平衡条件、Gibbs-Thomson 条件、熵守恒条件、溶质守恒条件和界面分离条件. 各向异性表面张力用四重对称函数 $\gamma(\theta) = \gamma_0(1 + \alpha_4 \cos 4\theta)$ 表示, 其中 γ_0 为各向同性表面张力参数, θ 为界面法向量与 Oy 轴之间的夹角, α_4 为表面张力各向异性的强度. 本文忽略固相中的热扩散和溶质扩散, 并假设深胞晶尖端曲率半径 ℓ_t 远小于溶质扩散长度 $\ell_D = \kappa_D/V$, 即 $\ell_t \ll \ell_D$, 其中 κ_D 为溶质扩散系数, 定义主间距参数 $W = \ell_w/\ell_t$, 其中 ℓ_w 为胞晶列的周期. 为了作渐近分析, 选取 ℓ_t 为长度尺度, 拉速 V 为速度尺度, ℓ_t/V 为时间尺度, $\Delta H/(c_p \rho)$ 为温度尺度, 其中 ΔH 为单位体积内固相潜热, c_p 为比热, ρ 为熔体密度, 于是深胞晶生长满足的热传导方程、溶质扩散方程以及界面条件转化为无量纲的控制方程. 进一步选取 $\varepsilon = \ell_t/\ell_D$ 为小参数. 由于深胞晶界面形态的周期性, 我们只需研究胞晶界面单个周期的界面形态. 与文献[14]一样, 利用 Saffman-Taylor 解构造曲线坐标系 (ξ, η) , 它与平面直角坐标系的关系为

$$x = WX(\xi, \eta) = W\lambda_0\xi - \frac{2W(1 - \lambda_0)}{\pi} \times \arctan\left(\frac{(1 - e^{\pi\eta}) \sin(\pi\xi)}{(\cos(\pi\xi) + 1)(1 + e^{\pi\eta})}\right),$$

$$y = WY(\xi, \eta) = W(2\lambda_0 - 1)\eta + \frac{W(1 - \lambda_0)}{\pi}$$

$$\times \ln \frac{e^{2\pi\eta} + 2e^{\pi\eta} \cos(\pi\eta) + 1}{4}, \quad (1)$$

其中 λ_0 是与主间距参数 W 有关的待定常数. 在曲线坐标系 (ξ, η) 下, 界面形状表示为 $\eta_B = \eta_B(\xi, \varepsilon)$, 它在胞晶尖端 $\xi = \eta = 0$ 处满足

$$\frac{\partial \eta_B}{\partial \xi}(0) = 0, \quad \eta_B(0) = 0, \quad (2)$$

在根部底端 $\xi = \pm 1$, $\eta = \eta_b$ 处满足

$$\eta_B(\pm 1) = \eta_b, \quad \frac{\partial \eta_B}{\partial \xi}(\pm 1) = 0. \quad (3)$$

液相温度分布近似为仅关于 y 的线性函数

$$T_L = \varepsilon G(y - y_0) + O(\varepsilon^2) \\ = \varepsilon G(WY(\xi, \eta) - y_0) + O(\varepsilon^2), \quad (4)$$

其中 y_0 是坐标原点到使温度 $T_L = 0$ 的点之间的距离, $G = (\ell_D G_T)/(\Delta H/(c_p \rho L))$ 为界面无量纲温度梯度. 可以看出, (4) 式满足热传导方程和热平衡条件. 在曲线坐标系 (ξ, η) 下, 溶质扩散方程表示为

$$\frac{\partial^2 C}{\partial \xi^2} + \frac{\partial^2 C}{\partial \eta^2} + \varepsilon W \left(Y_\xi \frac{\partial C}{\partial \xi} + X_\xi \frac{\partial C}{\partial \eta} \right) = 0. \quad (5)$$

方程(5)在界面上满足 Gibbs-Thomson 条件和溶质守恒条件:

$$C(\xi, 0) + \eta_B \frac{\partial C}{\partial \eta}(\xi, 0) \\ = y_* - \varepsilon \lambda_G W (Y(\xi, 0) + \eta_B Y_\eta(\xi, 0)) \\ - \frac{\varepsilon^2 \hat{\Gamma}}{MW_0} \left[(1 - \alpha_4 B_0(\xi) - \alpha_4 B_1(\xi) \eta_B \right. \\ \left. - \alpha_4 B_2(\xi) \eta'_B) K_0(\xi) - \frac{1}{G_0(\xi, 0)} \eta''_B ((1 \right. \\ \left. - \alpha_4 B_0(\xi)) + \alpha_4 B_1(\xi) \eta_B + \alpha_4 B_2(\xi) \eta'_B) \right], \quad (6)$$

$$\frac{\partial C}{\partial \eta}(\xi, 0) + \eta_B \frac{\partial^2 C}{\partial \eta^2}(\xi, 0) - \frac{\partial \eta_B}{\partial \xi} \frac{\partial C}{\partial \xi}(\xi, 0) \\ - \varepsilon W(1 - k) \left(C(\xi, 0) + \eta_B \frac{\partial C}{\partial \eta}(\xi, 0) \right) \\ \times \left(Y_\xi(\xi, 0) \frac{\partial \eta_B}{\partial \xi} - Y_\eta(\xi, 0) - Y_{\eta\eta}(\xi, 0) \eta_B \right) = 0, \quad (7)$$

其中 $\hat{\Gamma} = \varepsilon^{-2} \Gamma$, $\hat{\Gamma} = O(1)$, $\Gamma = \ell_c/\ell_t$ 为表面张力参数, $\ell_c = (\gamma c_p \rho T_M)/(\Delta H)^2$ 为毛细长度, T_M 为纯物质熔体温度, $M = -m C_\infty / (\Delta H / (c_p \rho))$ 为形态数, m 为相图中液相线斜率, $m < 0$, $\lambda_G = G/M$ 为长度比参数, 假设 $y_* = \varepsilon \lambda_G y_0$, κ 是分离系数,

$$G_0 = G(\xi, 0) = \sqrt{\lambda_0^2 + (1 - \lambda_0)^2 \tan^2 \frac{\pi \xi}{2}},$$

$$K_0(\xi) = \frac{\pi\lambda_0(1-\lambda_0)\cos\frac{\pi\xi}{2}}{2\left(\lambda_0^2 + (1-2\lambda_0)\sin^2\frac{\pi\xi}{2}\right)^{3/2}},$$

$$B_0(\xi) = \frac{a_1 - 2a_2\cos(\pi\xi) + a_3\cos^2(\pi\xi)}{(a_4 + a_5\cos(\pi\xi))^2},$$

$$B_1(\xi) = \frac{1}{(a_4 + a_5\cos(\pi\xi))^3} [16\pi\lambda_0(1-\lambda_0)^3 \times (1-\cos(\pi\xi))(a_4\cos(\pi\xi) + a_5)],$$

$$B_2(\xi) = \frac{16\lambda_0(1-\lambda_0)\sin(\pi\xi)(a_4\cos(\pi\xi) + a_5)}{(a_4 + a_5\cos(\pi\xi))^2},$$

$$a_1 = 1 - 4\lambda_0 + 8\lambda_0^3 - 4\lambda_0^4,$$

$$a_2 = 1 - 4\lambda_0 + 6\lambda_0^2 - 4\lambda_0^3,$$

$$a_3 = 1 - 4\lambda_0 + 12\lambda_0^2 - 16\lambda_0^3 + 8\lambda_0^4,$$

$$a_4 = 2\lambda_0^2 - 2\lambda_0 + 1, \quad a_5 = 2\lambda_0 - 1.$$

在单个胞晶的侧壁上, $\xi = \pm 1$,

$$\frac{\partial C}{\partial \xi}(\pm 1, \eta) = 0, \quad (8)$$

在远场处, $\eta \rightarrow \infty$ 时,

$$C \sim 1 + Q_0 e^{-\varepsilon W \eta}, \quad (9)$$

其中 Q_0 是与变量 ξ, η 无关的常数.

3 问题的渐近解和分析

方程(1)–(9)构成一个摄动问题, 当 $\varepsilon \rightarrow 0$ 时, 我们求出胞晶生长界面形态的渐近解. 与 Chen 等^[14]的分析一样, 将胞晶生长区域划分为远离根部的外部区域(I) 和根部附近的根部区域(II), 在外部区域和根部附近的根部区域分别求出渐近解, 然后将它们匹配得到在整个区域一致有效的渐近解.

3.1 外部区域的渐近解

先求在远离根部的外部区域(I) 的渐近解. 因为问题(2)–(9)是线性非齐次的, 所以将解分为非齐次问题的特解与对应的齐次问题的通解之和, 即

$$\{C, \eta_B\} = \{\bar{C}, \bar{\eta}_B\} + \{\tilde{C}, \tilde{\eta}_B\}. \quad (10)$$

这里 $\{\bar{C}, \bar{\eta}_B\}$ 表示非齐次问题的特解, $\{\tilde{C}, \tilde{\eta}_B\}$ 表示对应齐次问题的通解.

对于求非齐次问题的特解 $\{\bar{C}, \bar{\eta}_B\}$, 引入慢变量 $\tilde{\eta} = \varepsilon\eta$, 将浓度场看作为相互独立变量 $(\xi, \eta, \tilde{\eta})$

的多变量函数, 设 $\{\bar{C}, \bar{\eta}_B\}$ 的渐近展开为^[14]

$$\bar{C} = \bar{C}_0(\xi, \eta, \tilde{\eta}) + \varepsilon\bar{C}_1(\xi, \eta, \tilde{\eta}) + \dots, \quad (11)$$

$$\bar{\eta}_B(\xi, \varepsilon) = \varepsilon h_1(\xi) + \varepsilon^2 h_2(\xi) + \dots, \quad (12)$$

同时设

$$y_* = y_{*0} + \varepsilon y_{*1} + \dots, \quad (13)$$

$$W = W_0 + \varepsilon W_1 + \dots, \quad (14)$$

将式(11)–(14)代入到方程(2)–(9)依次得到如下的各级渐近解:

$$\bar{C}_0 = 1 + (y_{*0} - 1) e^{-W_0\tilde{\eta}}, \quad (15)$$

$$\begin{aligned} \bar{C}_1 &= W_0\lambda_G\eta - W_0\lambda_G Y(\xi, \eta) \\ &\quad + [y_{*1} e^{-W_0\tilde{\eta}} + W_0\lambda_G\beta_0 \\ &\quad \times (1 - e^{-W_0\tilde{\eta}})], \end{aligned} \quad (16)$$

$$h_1(\xi) = \sum_{m=0}^{\infty} B_{1,m} \cos(m\pi\xi), \quad (17)$$

$$\begin{aligned} y_{*0} &= \frac{1 + \lambda_G(1 - \lambda_0)}{1 - \lambda_0(1 - \kappa)}, \\ y_{*1} &= \frac{W_0\beta_0\lambda_0\lambda_G\kappa}{1 - (1 - \kappa)\lambda_0}, \end{aligned} \quad (18)$$

$$W_0 = \pi(1 - \lambda_0)/2\lambda_0^2, \quad (19)$$

$$W_1 = -\eta''_B(0)/\lambda_0, \quad (19)$$

其中 $\beta_0 = -(2\ln 2)(1 - \lambda_0)/\pi$, $B_{1,m}$ 满足线性方程组

$$\begin{aligned} \sum_{n=1}^{\infty} \hat{\phi}_{m,n} B_{1,n} - \frac{\lambda_0}{2(1 - \lambda_0)} B_{1,m} \\ = \frac{\lambda_0}{2W_0(1 - \lambda_0)\Delta_0} \left[(1 - \kappa)W_0^2\lambda_0\lambda_G\frac{\tau_m}{m\pi} \right. \\ \left. - \frac{\hat{\Gamma}}{MW_0}(\gamma_m - \alpha_4 S_m) - E_{2,m}(0, 0) \right. \\ \left. - \frac{1}{m\pi} \frac{\partial E_{2,m}}{\partial \eta}(0, 0) \right], \end{aligned} \quad (20)$$

$$S_m = \int_{-1}^1 [B_0(\xi)K_0(\xi) \cos(m\pi\xi)] d\xi,$$

$$\gamma_m = \int_{-1}^1 K_0(\xi) \cos(m\pi\xi) d\xi,$$

$$\tau_m = \int_{-1}^1 Y(\xi, 0) \cos(m\pi\xi) d\xi,$$

$$E_{2,m} = \frac{1}{2}W_0^2\lambda_G \int_{-1}^1 Y^2(\xi, 0) \cos(m\pi\xi) d\xi,$$

$$\frac{\partial E_{2,m}}{\partial \eta} = W_0^2 \left(\lambda_0\lambda_G + \frac{1}{2}\Delta_0 \right) \tau_m,$$

$$\Delta_0 = \lambda_0[(1 - \kappa)y_{*0} - \lambda_G],$$

$$\hat{\phi}_{m,n} = \begin{cases} 0, & (n > m), \\ (-1)^{m+n+1} 2, & (n < m), \\ -1 & (n = m). \end{cases} \quad (21)$$

为了求(10)式中对应齐次问题的通解 $\{\tilde{C}, \tilde{\eta}_B\}$, 引入快变量 ξ_+ 和 η_+ ^[14],

$$\begin{aligned} \xi_+ &= \frac{1}{\sqrt{\varepsilon \hat{F}}} \int_0^\xi k(\xi_1, \eta) d\xi_1, \\ \eta_+ &= \frac{1}{\sqrt{\varepsilon \hat{F}}} \int_0^\eta k(\xi, \eta_1) d\eta_1, \end{aligned}$$

其中

$$\begin{aligned} k(\xi, \eta) &= k_0(\xi, \eta) + \varepsilon k_1(\xi, \eta) + \dots, \\ k_0(\xi, 0) &= \bar{k}_0(\xi). \end{aligned}$$

将问题看成多重变量 $(\xi, \eta, \xi_+, \eta_+)$ 的函数, 当 $\varepsilon \rightarrow 0$ 时,

$$\begin{aligned} \tilde{C}(\xi, \eta, \varepsilon) &= \varepsilon \tilde{C}_0(\xi, \eta, \xi_+, \eta_+) \\ &\quad + \varepsilon^2 \tilde{C}_1(\xi, \eta, \xi_+, \eta_+) + \dots, \end{aligned} \quad (22)$$

$$\tilde{\eta}_B(\xi, \varepsilon) = \tilde{h}_0(\xi, \xi_+) + \varepsilon \tilde{h}_1(\xi, \xi_+) + \dots, \quad (23)$$

代入方程(2)—(9), 得到首阶项满足的方程

$$\frac{\partial^2 \tilde{C}_0}{\partial \xi_+^2} + \frac{\partial^2 \tilde{C}_0}{\partial \eta_+^2} = 0. \quad (24)$$

在胞晶侧壁 $\xi = \pm 1$ 上,

$$\frac{\partial \tilde{C}_0}{\partial \xi_+} = 0. \quad (25)$$

在界面上, 当 $\eta = \eta_+ = 0$ 时,

$$\begin{aligned} \tilde{C}_0 &= \frac{[1 - \alpha_4 B_0(\xi)] \bar{k}_0^2}{W_0 M G_0(\xi, 0)} \frac{\partial^2 \tilde{h}_0}{\partial \xi_+^2} \\ &\quad + \left\{ W_0 \Delta_0 - \frac{\alpha_4 B_1(\xi) \bar{k}_0^2}{W_0 M G_0(\xi, 0)} \right. \\ &\quad \times \left. \frac{\partial^2 \tilde{h}_0}{\partial \xi_+^2} - \frac{\partial \tilde{C}_0}{\partial \eta} \right\} \tilde{h}_0, \end{aligned} \quad (26)$$

$$\bar{k}_0 \frac{\partial \tilde{C}_0}{\partial \eta_+} = W_0 \frac{\Delta_0}{\lambda_0} Y_{\xi, 0}(\xi, 0) \bar{k}_0 \frac{\partial \tilde{h}_0}{\partial \xi_+}. \quad (27)$$

方程(24)—(26)有如下形式的模式解:

$$\begin{aligned} \tilde{C}_0 &= \bar{A}_0(\xi, \eta) e^{i\xi_+ - \eta_+}, \\ \tilde{h}_0 &= \bar{D}_0 \exp\{i\xi_+\}, \end{aligned} \quad (28)$$

其中 \bar{D}_0 为常数,

$$\bar{k}_0^3 = \bar{k}_0 W_0^2 M \Delta_0 G_0(\xi, 0) \frac{1 + \frac{i}{\lambda_0} Y_{\xi, 0}(\xi, 0)}{1 - \alpha_4 B_0(\xi)}, \quad (29)$$

方程(29)有三个根

$$\bar{k}_0^{(1)} = \bar{k}_s(\xi), \quad \bar{k}_0^{(2)} = -\bar{k}_s(\xi), \quad \bar{k}_0^{(3)} = 0,$$

其中

$$\bar{k}_s(\xi) = W_0 \sqrt{\frac{M \Delta_0 G_0(\xi, 0)}{[1 - \alpha_4 B_0(\xi)]}} \left[1 + \frac{i}{\lambda_0} Y_{\xi, 0}(\xi, 0) \right]^{1/2}.$$

记

$$\chi(\xi) = \int_0^\xi \bar{k}_s(\xi_1) d\xi_1 = \chi_R(\xi) + i\chi_I(\xi),$$

令 $\operatorname{Re}\{\bar{k}_s(\xi)\} > 0$, 则界面有三个基本解,

$$H_1(\xi) = e^{\frac{i}{\sqrt{\varepsilon \hat{F}}} \chi(\xi)}, \quad H_2(\xi) = e^{-\frac{i}{\sqrt{\varepsilon \hat{F}}} \chi(\xi)},$$

$$H_3(\xi) = 1.$$

注意到 $\operatorname{Im}\{\bar{k}_s(\xi)\} > 0$ ($-1 < \xi \leq 0$), 在远离界面处, 随着 η 的增加, 相应的浓度场趋于无穷, 不满足远场衰减条件, 所以必须剔除 $H_1(\xi)$. 又当 $\xi \rightarrow -1$ 时, $\operatorname{Re}\{\bar{k}_s(\xi)\} \rightarrow +\infty$ 和 $\operatorname{Im}\{\bar{k}_s(\xi)\} \rightarrow +\infty$, 这说明当 $\xi \rightarrow -1$ 时, $|H_2(\xi)| \rightarrow 0$, 从而得到外部区域的界面形状的外解

$$\begin{aligned} \eta_B(\xi, \varepsilon) &= \varepsilon \left[h_1(\xi) - h_1(0) e^{\frac{\chi_I(\xi)}{\sqrt{\varepsilon \hat{F}}}} \cos \left(\frac{\chi_R(\xi)}{\sqrt{\varepsilon \hat{F}}} \right) \right] \\ &\quad + \dots, \end{aligned} \quad (30)$$

界面上的浓度表示为

$$\begin{aligned} C(\xi, 0) &= y_{*0} + \varepsilon (y_{*1} - W_0 \lambda_G Y(\xi, 0)) \\ &\quad - \varepsilon^2 h_1(0) \left\{ W_0 \Delta_0 - \frac{[1 - \alpha_4 B_0(\xi)] \bar{k}_0^2(\xi)}{W_0 M G_0(\xi, 0)} \right\} \\ &\quad \times e^{\frac{\chi_I(\xi)}{\sqrt{\varepsilon \hat{F}}}} \cos \left(\frac{\chi_R(\xi)}{\sqrt{\varepsilon \hat{F}}} \right) + \dots. \end{aligned} \quad (31)$$

图1和图2分别显示了界面函数 $\eta_B(\xi)$ 和浓度的外解在各向异性表面张力作用下的变化. 随着各向异性表面张力增大胞晶前端部分收缩, 这说明胞晶前端的溶质容易向外排出.

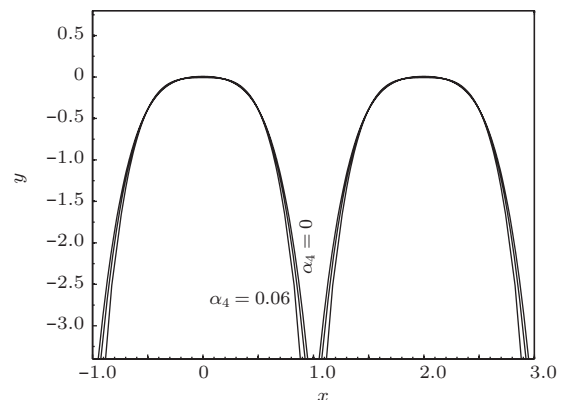


图1 各向异性表面张力影响下界面外解 $\eta_B(\xi)$ 表示的胞晶形态变化, 其中 $\varepsilon = 0.1$, $\kappa = 0.1$, $\lambda_G = 2.0$, $\lambda_0 = 0.6$, $M = 1.0$, $\hat{F} = 1.0$, $\alpha_4 = 0, 0.03, 0.06$ (从胞晶外向胞晶内)

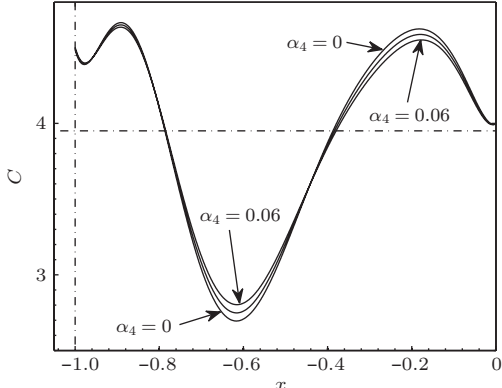


图2 界面上浓度受各向异性表面张力的影响, 其中 $\alpha_4 = 0, 0.03, 0.06, \varepsilon = 0.1, \kappa = 0.1, \lambda_G = 2.0, \lambda_0 = 0.6, M = 1.0, \hat{\Gamma} = 1.0$.

3.2 根部区域的渐近解

界面形状外解式(30)满足尖端光滑条件 $\eta_B(0) = \eta'_B(0) = 0$, 但是在 $\xi = \mp 1$ 处不满足根部光滑条件, 因此远离根部的外部区域(I)的渐近解, 但它不能提供关于根部底端的位置、胞晶的全长和根部底端的浓度信息. 为了求出根部附近的根部区域(II)的一致有效渐近解, 在根部区域 $|\xi + 1| \ll 1, |\eta - \eta_T(\xi)| \ll 1$, 假定函数 $\eta = \eta_T(\xi)$ 为根部区域的界面形状函数, 引入变量 $\hat{\xi}$ 和 $\hat{\eta}$ ^[14]:

$$\hat{\xi} = (1 + \xi)/\delta(\varepsilon), \quad \hat{\eta} = (\eta - \eta_T(\xi))/\delta(\varepsilon), \quad (32)$$

则在根部区域的远场处有 $\eta_B(\xi) \approx \varepsilon a_0(\xi \pm 1)^\alpha$, 其中 a_0 为常数.

为了使得根部区域的界面形状函数与外解(30)匹配, 需要根部区域的界面形状函数在根部区域的远场处满足条件

$$\eta_T(\xi) = \delta(\varepsilon)\hat{\eta}_T(\hat{\xi}) = \varepsilon a_0(1 + \xi)^\alpha = \varepsilon a_0 \delta^\alpha(\varepsilon) \xi_*^\alpha,$$

其中

$$\delta(\varepsilon) = \varepsilon^{\frac{1}{1-\alpha}},$$

$$\hat{\eta}_T(\hat{\xi}) = \begin{cases} \hat{\eta}_*, & (\xi_* < \hat{\xi} < \infty), \\ \hat{\eta}_b + a_2 \hat{\xi}^2 + a_3 \hat{\xi}^3, & (0 \leq \hat{\xi} < \xi_*), \end{cases}$$

这里 $\hat{\eta}_*$, $\hat{\eta}_b$, a_2 和 a_3 为 ξ_* 的函数:

$$\hat{\eta}_* = a_0 \xi_*^\alpha,$$

$$\hat{\eta}_b = a_0 [1 - \alpha(5 - \alpha)/6] \xi_*^\alpha,$$

$$a_2 = \frac{1}{2} a_0 \alpha(3 - \alpha) \xi_*^{\alpha-2},$$

$$a_3 = -\frac{1}{3} a_0 \alpha(2 - \alpha) \xi_*^{\alpha-3},$$

而 ξ_* 为待定的特征值. 假定根部区域界面形态函数 $|\hat{\eta}_B(\hat{\xi}, \varepsilon)| \ll 1$, 在界面 $\hat{\eta}_T(\hat{\xi})$ 附近界面形态函数表达为

$$\hat{\eta}_B(\hat{\xi}, \varepsilon) = \delta(\varepsilon) (\hat{\eta}_T(\hat{\xi}) + \hat{\eta}_B(\hat{\xi}, \varepsilon) + \dots), \quad (33)$$

在根部区域, 浓度场在内变量 $\{\hat{\xi}, \hat{\eta}\}$ 条件下可以表示为 $C = \hat{C}(\hat{\xi}, \hat{\eta}, \varepsilon)$, 应用根部变量, 将控制方程(4)式转化为如下形式的内部方程:

$$\begin{aligned} & \frac{\partial^2 \hat{C}}{\partial \hat{\xi}^2} + \left[1 + \hat{\eta}_T'^2(\hat{\xi}) \right] \frac{\partial^2 \hat{C}}{\partial \hat{\eta}^2} - 2\hat{\eta}_T'(\hat{\xi}) \frac{\partial^2 \hat{C}}{\partial \hat{\xi} \partial \hat{\eta}} \\ & - \hat{\eta}_T''(\hat{\xi}) \frac{\partial \hat{C}}{\partial \hat{\eta}} + \varepsilon W \left\{ \hat{Y}_{\hat{\xi}} \frac{\partial \hat{C}}{\partial \hat{\xi}} + \left[\hat{X}_{\hat{\xi}} \right. \right. \\ & \left. \left. - \hat{Y}_{\hat{\xi}} \hat{\eta}_T'(\hat{\xi}) \right] \frac{\partial \hat{C}}{\partial \hat{\eta}} \right\} = 0. \end{aligned} \quad (34)$$

匹配条件 $\hat{\eta} \rightarrow \infty$ 时, $\hat{C} \Leftrightarrow \bar{C}$.

侧壁条件 $\hat{\xi} = 0$ 时, $\frac{\partial \hat{C}}{\partial \hat{\xi}} = 0$.

在界面上, \hat{C} 满足在 $\hat{\eta} = 0$ 处线性化的界面条件:

$$\begin{aligned} & \hat{C} + \frac{\partial \hat{C}}{\partial \hat{\eta}} \hat{\eta}_B \\ & = y_* - \varepsilon \ln \delta(\varepsilon) W \lambda_G \hat{Y}_* - \varepsilon W \lambda_G \left(\hat{Y}_0 + \delta(\varepsilon) \hat{Y}_1 \right) \\ & - \varepsilon W \lambda_G \frac{\partial \hat{Y}_0}{\partial \hat{\eta}} \hat{\eta}_B + \frac{\varepsilon^2 \pi \hat{\Gamma}}{2WM(1 - \lambda_0)} \frac{\hat{\eta}_T}{\sqrt{\hat{\xi}^2 + \hat{\eta}_T^2}} \\ & \times \left(1 - \alpha_4 + \frac{8\pi\alpha_4\lambda_0\delta(\varepsilon)}{1 - \lambda_0} \hat{\eta}_B \right) - \frac{\varepsilon^2 \hat{\Gamma}}{WM \hat{G}_0(\xi, 0)} \\ & \times \left(1 - \alpha_4 - \frac{8\pi\alpha_4\lambda_0\delta(\varepsilon)}{1 - \lambda_0} \hat{\eta}_B \right) \hat{\eta}_B'', \end{aligned} \quad (35)$$

$$\begin{aligned} & \frac{\partial \hat{C}}{\partial \hat{\eta}} + \frac{\partial^2 \hat{C}}{\partial \hat{\eta}^2} \hat{\eta}_B - \frac{\partial \hat{\eta}_B}{\partial \hat{\xi}} \frac{\partial \hat{C}}{\partial \hat{\xi}} - \varepsilon W(1 - \kappa) \\ & \times \left(\hat{C} + \frac{\partial \hat{C}}{\partial \hat{\eta}} \hat{\eta}_B \right) \left(\hat{Y}_{\hat{\xi}, 0} \frac{\partial \hat{\eta}_B}{\partial \hat{\xi}} - \hat{Y}_{\hat{\eta}, 0} \right) \\ & + \varepsilon W(1 - \kappa) \left(\hat{C} + \frac{\partial \hat{C}}{\partial \hat{\eta}} \hat{\eta}_B \right) \hat{Y}_{\hat{\eta}, 0} \hat{\eta}_B = 0, \end{aligned} \quad (36)$$

其中

$$\hat{Y}_* = \frac{2(1 - \lambda_0)}{\pi},$$

$$\hat{Y}_0 = \frac{(1 - \lambda_0)}{\pi} \ln \frac{\pi^2 \left[(\hat{\eta} + \hat{\eta}_T)^2 + \hat{\xi}^2 \right]}{4},$$

$$\hat{Y}_1 = \lambda_0 (\hat{\eta} + \hat{\eta}_T),$$

$$\hat{Y}_{\hat{\eta}, 0}(\hat{\xi}, \hat{\eta}) = \frac{2(1 - \lambda_0)}{\pi} \frac{\hat{\eta} + \hat{\eta}_T}{\hat{\xi}^2 + (\hat{\eta} + \hat{\eta}_T)^2},$$

$$\begin{aligned}\hat{Y}_{\hat{\eta},1}(\hat{\xi}, \hat{\eta}) &= \lambda_0, \\ \hat{Y}_{\hat{\xi},0}(\hat{\xi}, \hat{\eta}) &= \frac{2(1-\lambda_0)}{\pi} \frac{\hat{\xi}}{\hat{\xi}^2 + (\hat{\eta} + \hat{\eta}_T)^2}, \\ \hat{G}_0(\hat{\xi}, \hat{\eta}) &= \frac{2(1-\lambda_0)}{\pi} \frac{1}{\sqrt{\hat{\xi}^2 + (\hat{\eta} + \hat{\eta}_T)^2}}, \\ \hat{K}_0(\hat{\xi}, 0) &= -\frac{\pi}{2(1-\lambda_0)} \frac{\hat{\eta}_T}{\sqrt{\hat{\xi}^2 + \hat{\eta}_T^2}}.\end{aligned}$$

非齐次方程系统(34)–(36)的解有两部分:

$$\begin{aligned}&\left\{ \hat{C}(\hat{\xi}, \hat{\eta}, \varepsilon), \hat{\eta}_B(\hat{\xi}, \varepsilon) \right\} \\ &= \left\{ \bar{C}_*(\hat{\xi}, \hat{\eta}, \varepsilon), \bar{h}_*(\hat{\xi}, \varepsilon) \right\} \\ &\quad + \left\{ \tilde{C}_*(\hat{\xi}, \hat{\eta}, \varepsilon), \tilde{h}_*(\hat{\xi}, \varepsilon) \right\},\end{aligned}\quad (37)$$

其中 $\{\bar{C}_*, \bar{h}_* = 0\}$ 部分为非齐次系统的特解, $\{\tilde{C}_*, \tilde{h}_*\}$ 部分为齐次部分的通解.

非齐次系统的特解 \bar{C}_* 直接由正则展开法得到

$$\begin{aligned}\bar{C}_*(\hat{\xi}, \hat{\eta}, \varepsilon) &= y_{*0} - \varepsilon \ln \delta(\varepsilon) \hat{Y}_* \\ &+ \varepsilon \left[y_{*1} - W_0 \lambda_G Y_0(\hat{\xi}, \hat{\eta}) \right] + \dots\end{aligned}\quad (38)$$

为求齐次部分的通解 $\{\tilde{C}_*, \tilde{h}_*\}$, 引进内部快变量

$$\begin{aligned}\tilde{\xi}_+ &= \frac{\tilde{\phi}(\hat{\xi}, \hat{\eta})}{\sqrt{\varepsilon \hat{\Gamma}}} = \frac{1}{\sqrt{\varepsilon \hat{\Gamma}}} \int_0^{\hat{\xi}} \tilde{k}(\hat{\xi}_1, \hat{\eta}) d\hat{\xi}_1, \\ \tilde{\eta}_+ &= \frac{\tilde{\varphi}(\hat{\xi}, \hat{\eta})}{\sqrt{\varepsilon \hat{\Gamma}}} = \frac{1}{\sqrt{\varepsilon \hat{\Gamma}}} \int_0^{\hat{\eta}} \tilde{g}(\hat{\xi}, \hat{\eta}_1) d\hat{\eta}_1,\end{aligned}\quad (39)$$

设(34)–(36)有渐近展开解

$$\tilde{C}_* = \varepsilon \tilde{b}_{*0} \tilde{C}_{*0}(\hat{\xi}, \hat{\eta}, \tilde{\xi}_+, \tilde{\eta}_+) + \dots, \quad (40)$$

$$\hat{\eta}_B(\hat{\xi}, \varepsilon) = \tilde{b}_{*0}(\varepsilon) \tilde{h}_{*0}(\hat{\xi}, \tilde{\xi}_+) + \dots, \quad (41)$$

其中 $\tilde{b}_{*0}(\varepsilon)$ 为待定函数, 代入(34)–(36)式, 得到首项 \tilde{C}_{*0} 满足方程

$$\frac{\partial^2 \tilde{C}_{*0}}{\partial \tilde{\xi}_+^2} + \frac{\partial^2 \tilde{C}_{*0}}{\partial \tilde{\eta}_+^2} = 0, \quad (42)$$

和如下的边界条件:

匹配条件: 当 $\hat{\eta} \rightarrow \infty$, $\xi \rightarrow -1$, $\eta \rightarrow 0$ 时,

$$\tilde{C}_{*0} \Leftrightarrow \tilde{C}_0; \quad (43)$$

关于 $\hat{\xi} = 0$ 的对称条件:

$$\tilde{C}_{*0}(\hat{\xi}, \hat{\eta}, \tilde{\xi}_+, \tilde{\eta}_+) = \tilde{C}_{*0}(-\hat{\xi}, \hat{\eta}, -\tilde{\xi}_+, \tilde{\eta}_+); \quad (44)$$

界面条件: 在界面 $\hat{\eta} = \tilde{\eta}_+ = 0$ 处,

$$\tilde{C}_{*0} = \frac{(1-\alpha_4) \hat{k}_0^2}{M W_0 \hat{G}_0(\hat{\xi}, 0)} \frac{\partial^2 \tilde{h}_{*0}}{\partial \tilde{\xi}_+^2}, \quad (45)$$

$$\begin{aligned}&\frac{\hat{k}_0}{\sqrt{1+\hat{\eta}_T^2}} \frac{\partial \tilde{C}_{*0}}{\partial \tilde{\eta}_+} \\ &= \hat{k}_0 W_0 \frac{\Delta_0}{\lambda_0} \hat{Y}_{\hat{\xi},0}(\hat{\xi}, 0) \frac{\partial \tilde{h}_{*0}}{\partial \tilde{\xi}_+}.\end{aligned}\quad (46)$$

方程(42)有正则模式解

$$\begin{aligned}\tilde{C}_{*0} &= \tilde{A}_{*0}(\xi, \eta) \exp\{i\tilde{\xi}_+ - \tilde{\eta}_+\}, \\ \tilde{h}_{*0} &= \tilde{D}_{*0} \exp\{i\tilde{\xi}_+\},\end{aligned}\quad (47)$$

其中 $\tilde{A}_{*0}(\xi, \eta)$ 是函数, \tilde{D}_{*0} 是常数, 将(42)式代入(45)和(46)得到 $\tilde{A}_{*0}(\xi, \eta)$ 和 \tilde{D}_{*0} 的特征值问题, $\hat{k}_0(\hat{\xi})$ 满足三次代数方程

$$\begin{aligned}&\frac{[1-\alpha_4]\hat{k}_0^3}{M W_0 \hat{G}_0(\hat{\xi}, 0) \sqrt{1+\hat{\eta}_T^2}} \\ &- i \hat{k}_0 W_0 \frac{\Delta_0}{\lambda_0} \hat{Y}_{\hat{\xi},0}(\hat{\xi}, 0) = 0,\end{aligned}\quad (48)$$

解得这方程 \hat{k}_0 的三个根

$$\begin{aligned}\hat{k}_0^{(1)}(\hat{\xi}) &= \hat{k}_S(\hat{\xi}), \quad \hat{k}_0^{(2)}(\hat{\xi}) = -\hat{k}_S(\hat{\xi}), \\ \hat{k}_0^{(3)}(\hat{\xi}) &= 0,\end{aligned}\quad (49)$$

其中

$$\begin{aligned}\hat{k}_S(\hat{\xi}) &= 2 e^{\frac{i\pi}{4}} \frac{W_0(1-\lambda_0)}{\pi} \sqrt{\frac{M \Delta_0}{\lambda_0}} \\ &\times \frac{\hat{\xi}^{1/2} (1+\hat{\eta}_T'^2)^{1/4}}{\left[1-\alpha_4 \hat{B}_0(\hat{\xi})\right]^{1/2} \left[\hat{\xi}^2 + \hat{\eta}_T^2(\hat{\xi})\right]^{3/4}}.\end{aligned}$$

记

$$\hat{\chi}(\hat{\xi}) = \int_{\xi_*}^{\hat{\xi}} \hat{k}_S(\hat{\xi}_1) d\hat{\xi}_1 = \hat{\chi}_R(\hat{\xi}) + i \hat{\chi}_I(\hat{\xi}),$$

则得根部区域界面形状函数解为

$$\begin{aligned}\hat{\eta}_B(\xi, \varepsilon) &= \delta(\varepsilon) \hat{\eta}_T(\hat{\xi}) - \varepsilon \Delta(\varepsilon) h_1(0) e^{-\frac{i}{\sqrt{\varepsilon \hat{\Gamma}}} \hat{\chi}(\hat{\xi})} \\ &+ \dots,\end{aligned}\quad (50)$$

其中

$$\begin{aligned}\Delta(\varepsilon) &= \exp \left\{ -W_0 \frac{(1-i)}{\sqrt{\varepsilon \hat{\Gamma}}} \frac{\sqrt{2}(1-\lambda_0)}{\pi} \sqrt{\frac{M \Delta_0}{\lambda_0}} \right. \\ &\times \left. \int_{\xi_*}^{\frac{1}{\delta(\varepsilon)}} \frac{\hat{\xi}_1^{1/2} (1+\hat{\eta}_T'^2)^{1/4} d\hat{\xi}_1}{(1-\alpha_4)^{1/2} (\hat{\xi}_1^2 + \hat{\eta}_T^2(\hat{\xi}_1))^{3/4}} \right\},\end{aligned}$$

函数(50)中 $\hat{\chi}(\hat{\xi})$ 满足量子化条件

$$-\operatorname{ctg} \left(\frac{\hat{\chi}_R(0)}{\sqrt{\varepsilon \hat{\Gamma}}} \right) = e^{-\frac{2\hat{\chi}_R(0)}{\sqrt{\varepsilon \hat{\Gamma}}}}, \quad (51)$$

从(51)式可解出一系列特征值 $\xi_* = \xi_*^{(0)} < \xi_*^{(1)} < \xi_*^{(2)} < \dots$, 它们是参数 α_4, ε 的函数. 图3显示最小的特征值 $\xi_* = \xi_*^{(0)}$ 随各向异性表面张力参数 α_4 增大而减小.

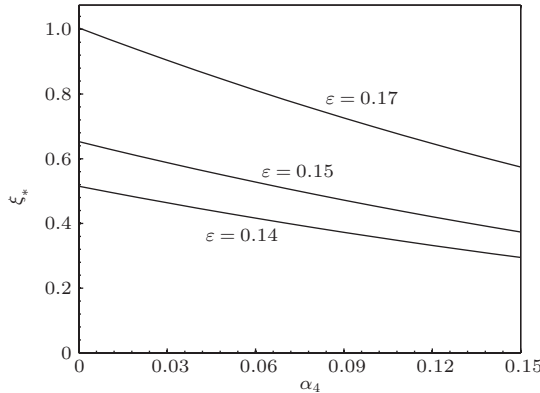


图3 特征值 ξ_* 随各向异性表面张力的变化, 其中 $\varepsilon = 0.14, 0.15, 0.17$ (从下到上), $\varepsilon = 0.1, \kappa = 0.1, \lambda_G = 2.0, \lambda_0 = 0.6, M = 1.0, \hat{\Gamma} = 1.0, \alpha = 0.86, a_0 = 2.4$

通过匹配方法将界面函数的外解和内解匹配, 得到界面函数的合成展开解

$$\begin{aligned} & \eta_B(\xi, \varepsilon) \\ &= \delta(\varepsilon) \hat{\eta}_T(\hat{\xi}) - \varepsilon a_0 (1 + \xi)^\alpha + \varepsilon h_1(\xi) \\ & \quad - \varepsilon h_1(0) \left[e^{\frac{\chi_I(\xi)}{\sqrt{\varepsilon \hat{\Gamma}}}} \cos \left(\frac{\chi_R(\xi)}{\sqrt{\varepsilon \hat{\Gamma}}} \right) \right. \\ & \quad \left. - \Delta(\varepsilon) e^{\frac{\hat{\chi}_I(\hat{\xi})}{\sqrt{\varepsilon \hat{\Gamma}}}} \cos \left(\frac{\hat{\chi}_R(\hat{\xi})}{\sqrt{\varepsilon \hat{\Gamma}}} \right) \right] + \dots \quad (52) \end{aligned}$$

根据上述所得到的根部解, 确定指状界面的振幅长度为

$$\begin{aligned} Y_b &= |Y(-1, \delta(\varepsilon) \hat{\eta}_b)| \approx \left| \ln \delta(\varepsilon) \hat{Y}_* + \hat{Y}_0(0, \hat{\eta}_b) \right| \\ &= \frac{2(1 - \lambda_0)}{\pi} \left| \ln \delta(\varepsilon) + \ln \left(\frac{\pi \hat{\eta}_b}{2} \right) \right|. \quad (53) \end{aligned}$$

根部底端的平均曲率为

$$K_b \approx -\pi (1 + 2a_2 \hat{\eta}_b) / 2(1 - \lambda_0). \quad (54)$$

在根部 $(\hat{\xi} = 0, \hat{\eta} = \hat{\eta}_b)$ 浓度为

$$\begin{aligned} C_{\text{root}} &= y_{*0} + \varepsilon \left(y_{*1} - W_0 \lambda_G \ln \delta(\varepsilon) \hat{Y}_* \right. \\ &\quad \left. - W_0 \lambda_G \hat{Y}_0(0, \hat{\eta}_b) \right) + \dots, \quad (55) \end{aligned}$$

其中 $\hat{Y}_0(0, \hat{\eta}_b) = [2(1 - \lambda_0) \ln(\pi \hat{\eta}_b / 2)] / \pi$, $\hat{Y}_* = 2(1 - \lambda_0) / \pi$.

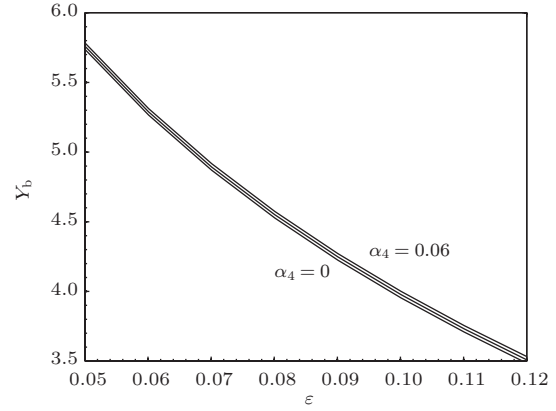


图4 胞晶指状界面的振幅对不同各向异性表面张力随参数 ε 的变化, 其中 $\alpha_4 = 0, 0.03, 0.06$ (从下到上), $\kappa = 0.1, \lambda_G = 2.0, \lambda_0 = 0.6, M = 1.0, \hat{\Gamma} = 1.0, \alpha = 0.86, a_0 = 2.4$

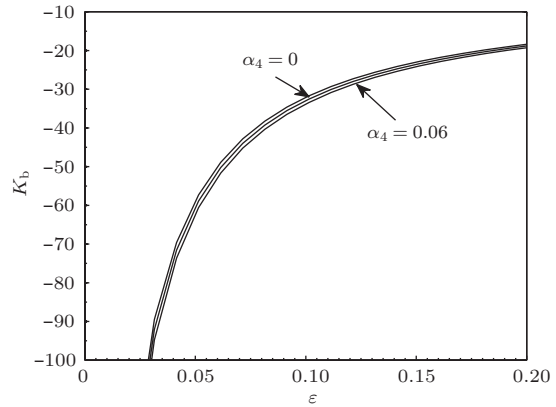


图5 胞晶根部底端的平均曲率对不同各向异性表面张力随参数 ε 的变化, 其中 $\alpha_4 = 0, 0.03, 0.06$ (从上到下), $\kappa = 0.1, \lambda_G = 2.0, \lambda_0 = 0.6, M = 1.0, \hat{\Gamma} = 1.0, \alpha = 0.86, a_0 = 2.4$

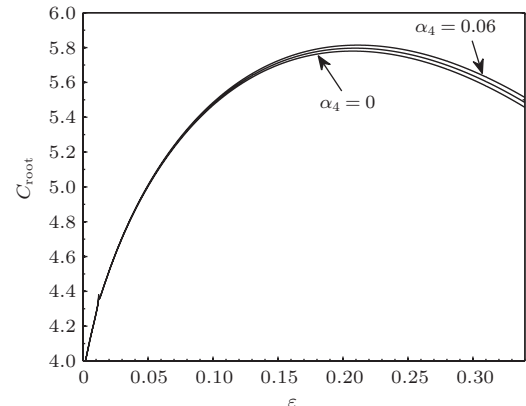


图6 浓度在根部随各向异性表面张力的变化, 其中 $\alpha_4 = 0, 0.03, 0.06$ (从下到上), $\kappa = 0.1, \lambda_G = 2.0, \lambda_0 = 0.6, M = 1.0, \hat{\Gamma} = 1.0, \alpha = 0.86, a_0 = 2.4$

图4和图5显示随着各向异性表面张力参数的增加胞晶界面振幅增加, 根部底端的曲率增大或

根部底端的曲率半径减小。图6显示随着各向异性表面张力参数 α_4 的增加胞晶指状界面的振幅增加, 根部底端的位置振幅增加, 根部底端的曲率 $|K_b|$ 增大, 或根部底端的曲率半径减小, 这说明胞晶根部的溶质不易排出。

4 结 论

本文利用匹配渐近展开法和多变量展开法求出定向凝固深胞晶生长的浓度场和界面形态的全局渐近解, 研究各向异性表面张力对定向凝固深胞晶生长的影响。本文结果能够计算定向凝固过程中深胞晶生长的浓度、界面形状。结果表明, 各向异性表面张力对定向凝固过程深胞晶生长有显著的影响, 随着各向异性表面张力增大, 胞晶前端部分浓度减小而胞晶界面收缩, 这说明胞晶前端的溶质容易向外排出; 胞晶根部的浓度增大而界面曲率增大或根部的曲率半径减小, 这说明胞晶根部的溶质不易排出。各向异性表面张力使得深胞晶界面振幅增加。本文结果能够计算定向凝固过程中深胞晶生长的浓度、界面形态。

据作者所知, 各向异性表面张力对于深胞晶界面的生长还未见详细的实验数据, 本文结果有待于实验进一步验证。

感谢加拿大麦吉尔大学和北京科技大学海外名师Xu Jian-Jun教授2013年访问北京科技大学时给予的指导帮助。

参考文献

- [1] Mullins W W, Sekerka R F 1964 *J. Appl. Phys.* **35** 444
- [2] Mullins W W, Sekerka R F 1963 *J. Appl. Phys.* **34** 323
- [3] Langer J S, Turski L A 1977 *Acta Metall.* **32** 1113
- [4] Corell S R, McFadden G B 1993 *Handbook of Crystal Growth* (Berlin: Springer-Verlag), Chapter 12 785
- [5] McFadden G B, Corell S R 1984 *Physica D* **12** 253
- [6] Coriell S R, McFadden G B 2002 *J. Crystal Growth* **237–239** 8
- [7] Boettinger W J, Coriell S R, Greer A L, Karma A, Kurz W, Rappaz M, Trivedi R 2000 *Acta Materialia* **48** 43
- [8] Xu J J 1998 *Interfacial wave theory of pattern formation* (Berlin: Springer-Verlag) pp79–242
- [9] Davis S H 2001 *Theory of Solidification* (Cambridge, UK: Cambridge University Press) pp42–214
- [10] Huang W D, Lin X, Li T, Wang L L 2004 *Acta Phys. Sin.* **57** 3978
- [11] Zhang Y P, Lin X, Wei L, Wang M, Peng D J, Huang W D 2012 *Acta Phys. Sin.* **61** 228106 (in Chinese)[张云鹏, 林鑫, 魏雷, 王猛, 彭东剑, 黄卫东 2012 物理学报 **61** 228106]
- [12] Weeks J D, van Saarloos W 1989 *Phys. Rev. A* **39** 2772
- [13] Weeks J D, van Saarloos W, Grant M 1991 *J. Crystal Growth* **112** 244
- [14] Chen Y Q, Xu J J 2011 *Phys. Rev. E* **83** 041601

Effect of anisotropic surface tension on deep cellular crystal growth in directional solidification*

Chen Ming-Wen^{1)†} Chen Yi-Chen¹⁾ Zhang Wen-Long¹⁾ Liu Xiu-Min¹⁾
Wang Zi-Dong^{2)‡}

1) (School of Mathematics and Physics, University of Science and Technology Beijing, Beijing 100083, China)

2) (School of Materials Science and Engineering, University of Science and Technology Beijing, Beijing 100083, China)

(Received 29 August 2013; revised manuscript received 5 November 2013)

Abstract

An asymptotic solution of the concentration and interface morphology for a deep cellular crystal in directional solidification is obtained by using the matched asymptotic expansion method and multiple variable expansion method, and the effect of anisotropic surface tension on deep cellular crystal growth is studied. Results show that the anisotropic surface tension has a significant effect on the concentration and interface shape of deep cellular crystal growth in directional solidification. As the anisotropic surface tension parameter increases, the concentration near the front part of deep cellular crystal decays and the interface shrinks; when as the concentration near the root increases and the curvature of the interface near the root increases or the curvature radius decreases; and the amplitude of the deep cellular crystal increases. The concentration and interface shape of the deep cellular crystal in directional solidification can be calculated with the results obtained in this paper.

Keywords: directional solidification, deep cellular crystal growth, anisotropic surface tension, asymptotic solution

PACS: 81.10.Aj, 81.30.Fb

DOI: 10.7498/aps.63.038101

* Project supported by the Overseas Distinguished Scholar Program by the Ministry of Education of the People's Republic of China (Grant No. MS2010BJKJ005), the National Natural Science Foundation of China (Grant No. 10972030), and the Fundamental Research Funds for the Central University (Grant No. FRF-BR-11-034B).

† Corresponding author. E-mail: chenmw@ustb.edu.cn

‡ Corresponding author. E-mail: wangzd@mater.ustb.edu.cn